Langmuir

Article

pubs.acs.org/Langmuir

Sulfidization of Au(111) from Thioacetic Acid: An Experimental and Theoretical Study

Jeison A. Fischer,[†] Vinícius C. Zoldan,[†] Guillermo Benitez,[‡] Aldo A. Rubert,[‡] Eduardo A. Ramirez,[‡] Pilar Carro,[§] Roberto C. Salvarezza,[‡] André A. Pasa,*[,†] and Maria E. Vela*[,‡]

[†]Laboratório de Filmes Finos e Superfícies, Departamento de Física, Universidade Federal de Santa Catarina, Florianópolis, SC, Brazil

[‡]Instituto de Investigaciones Fisicoquímicas Teóricas y Aplicadas (INIFTA), Universidad Nacional de La Plata—CONICET, La Plata, Argentina

[§]Departamento de Química Física, Instituto de Materiales y Nanotecnología, Universidad de La Laguna, Tenerife, Spain

Supporting Information

ABSTRACT: We have studied the adsorption of thioacetic acid (TAAH) on Au(111) from solution deposition. The close proximity of the SH groups to CO groups makes this molecule very attractive for exploring the effect of the functional group on the stability of the S−C and S−Au bonds. Although thioacetic acid was supposed to decompose slowly in water by hydrolysis supplying hydrogen sulfide, this behavior is not expected in nonpolar solvents such as toluene or hexane. Therefore, we have used these solvents for TAAH self-assembly on the Au(111) surface. The characterization of the adsorbates has been done by electrochemical techniques, X-ray photoelectron spectroscopy (XPS), and scanning tunneling microscopy (STM). We have found that even in nonpolar solvents thioacetic acid decomposes to S. The results have been discussed on the basis that the adsorbed species suffer a cleavage on the Au surface, leaving the S attached to it. The dissociation is a spontaneous process that reaches the final state very fast once it is energetically favorable, as can be interpreted from DFT calculations. The thioacetic acid adsorption reveals the strong effect that produces a functional group and the key role of the S−H bond cleavage in the self-assembly process.

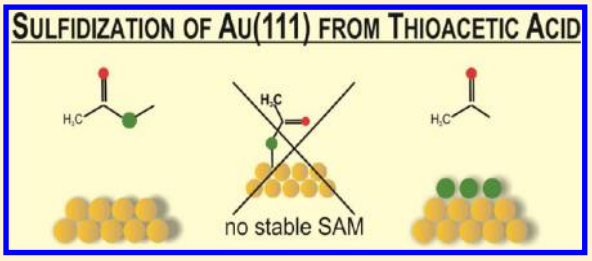

INTRODUCTION

Self-assembled monolayers (SAMs) of thiols on gold are an important system that allows an understanding of the interaction between organic molecules and metallic surfaces and can be used in a wide range of applications.[1] This system has the additional advantage that the preparation is simple and permits control of the surface properties. However, the possibility of introducing functional groups into organosulfur molecules has opened new challenges to describe the influence of these groups in the formation of the self-assembled monolayer and in the functionalities of the system.[2−4]

In general, the functional groups are not directly involved in the attachment of molecules to surfaces. They are widely used to control the surface chemistry (terminal groups) or to improve the intermolecular interactions that cause the SAM to be more stable (interchain cross-linking, hydrogen bonding, etc). In contrast, the influence of a functional group close to the reactive SH head has been much less studied in terms of the molecule reactivity, in particular, with respect to the C−S and S−Au bond strength and stability. This is not a minor point because recent work has also shown the formation of a sulfur (S) adlayer by the simple immersion of a gold substrate in a solution containing molecular precursors of sulfonyl,[5] disilathiane,[6] thioglucose,[7] and methylthiolate activated by oxidative dehydrogenation,[8] indicating the cleavage of S−C bonds catalyzed by Au.

In this work, we have studied the adsorption of thioacetic acid (TAAH, chart S1 in Supporting Information) on Au(111) from solution deposition. The close proximity of the SH groups to CO groups makes this molecule very attractive for exploring the effect of the functional group on the stability of the S−C and S−Au bonds. Although TAAH acid was supposed to decompose slowly in water by hydrolysis supplying H_2S,[9] this behavior is not expected in nonpolar solvents such as toluene and hexane. Therefore, we have used these solvents for TAAH self-assembly on the Au(111) surface. The characterization of the adsorbates has been done by electrochemical techniques, X-ray photoelectron spectroscopy (XPS), and scanning tunneling microscopy (STM). We have found that even in nonpolar solvents TAAH decompose to S. The results have been discussed on the basis that the adsorbed species suffer a cleavage on the Au surface, leaving the S attached to it. The dissociation is a spontaneous process that does not need intermediate compounds and reaches the final state very fast

Received: July 27, 2012
Revised: September 18, 2012
Published: September 24, 2012

once it is energetically favorable, as can be interpreted from DFT calculations.

EXPERIMENTAL METHODS

Evaporated Au films on glass with a (111) preferred orientation (AF 45 Berliner Glass KG, Germany) were used as substrates. The gold-on-glass substrates were made of 0.7-mm-thick borosilicate glass covered with a 2.5-nm-thick chromium adhesion layer and a 250-nm-thick final gold layer. For this work, the substrates were annealed with butane or a hydrogen flame for 3 min to produce flat terraces with a (111) preferred orientation. Thioacetic acid (TAAH) was purchased from Merck (purity ≥98%) and used as received. All other chemicals were of the best analytical grade available.

The samples were prepared by immersing the Au(111) substrates on a freshly prepared 0.1 mM TAAH solution in toluene for 5 min, 30 min, 1 h, 6 h, and 12 h at room temperature in the absence of light. Occasionally, the self-assembly process was also carried out in ethanol and hexane to determine the effect of the solvent on adlayer formation. All samples were rinsed with the solvent and dried with N_2 after removal from the solution.

Standard three-electrode electrochemical cells were employed with a potentiostat (Autolab PGSTAT 30) with data acquisition capabilities for the electrochemical measurements. A saturated calomel electrode (SCE) and a large-area platinum foil were used as reference and counter electrodes, respectively. All potentials in the text are referenced to the SCE scale. The base electrolyte, a 0.1 M NaOH aqueous solution, was prepared with Milli-Q water and solid NaOH (analytical grade from Sigma) and was degassed with purified nitrogen 15 min prior to the experiments. Reductive electrodesorption of the layers from the Au substrates was performed by a linear potential sweep at 50 mV s^{-1} in deaerated aqueous 0.1 M NaOH at room temperature.

XPS measurements were made with a Mg Kα source (1253.6 eV) from XR50, Specs GmbH, and a hemispherical electron energy analyzer from PHOIBOS 100, Specs GmbH. Spectra were acquired with a 10 eV pass energy. A two-point calibration of the energy scale was performed using gold cleaned by sputtering (Au $4f_{7/2}$, binding energy = 84.00 eV) and copper (Cu $2p_{3/2}$, binding energy = 933.67 eV) samples. C 1s at 285 eV was used as a charging reference. The spectra were fitted with the XPSPEAK 4.1 software package, using a Shirley-type background and Gaussian−Lorentzian functions. For the XPS experimental setup used in this work, the ratio of S/Au = 0.056 corresponds to $\theta = {}^1/_3$, as measured for several alkanethiols on gold.[2]

STM imaging was done in constant-current mode in air, either with a Nanoscope IIIa microscope from Veeco Instruments (Santa Barbara, CA) or with an SPM from Molecular Imaging. Commercial Pt−Ir tips that were mechanically cut were used for STM imaging. Typical tunneling currents, bias voltages, and scan rates were 0.1−1 nA, 200−1000 mV, and 3−24 Hz, respectively.

DENSITY FUNCTIONAL THEORY CALCULATIONS

Ab initio calculations were performed using periodic DFT with a plane-wave pseudopotential. The exchange-correlation potential was described by means of the generalized gradient approach (GGA) with the Perdew−Wang (PW91) implementation.[10] The one-electron wave functions have been expanded on a plane wave basis set with a cutoff of 450 eV for the kinetic energy. The projector augmented wave (PAW) method,[11,12] as implemented by Kresse and Joubert,[13] has been employed to describe the effect of the inner cores of the atoms on the valence electrons. Energy minimization (electronic density relaxation) for a given nuclear configuration was carried out using a Davidson block iteration scheme. The dipole correction was applied to minimize polarization effects caused by the asymmetry of the slabs. All calculations have been carried out using the VASP 5.2.11 package.[13,14] Long-range dispersion corrections have been taken into account within the DFT-D2 approach of Grimme[15] as implemented in that version of VASP. Because the gold atom is not described in the original paper by Grimme, we have used for the dispersion coefficient C_6 and the vdW radius R_0 19.73 J nm^6/mol and 1.497 Å, respectively.[16,17]

The Au(111) surface is modeled by a five-Au-layer-thick slab with an optimized bulk lattice parameter of 4.18 Å. The vacuum separation between periodically repeated slabs is ∼12 Å. Adsorption occurs on only one side of the slab. During the geometry optimization, the two bottom layers were kept fixed at their optimized bulk truncated geometry for the Au(111) surface. The three outermost atomic metal layers and the atomic coordinates of the adsorbed species were allowed to relax without further constraints. The atomic positions were relaxed until the force on the unconstrained atoms was less than 0.03 eV/ Å. The minimum-energy paths for the decomposition reactions were mapped out using the nudged elastic band (NEB) method developed by Jönsson and co-workers.[18,19]

The $(2 \times \sqrt{3})$ unit cell of the Au(111) surface was employed to describe the adsorption of TAAH molecule and the TAA moiety, whereas the (5×5) and $(\sqrt{3} \times \sqrt{3})$ R30° unit cells were for S adsorption. The 2D Brillouin zone integrals are performed according to the Monkhorst−Pack[20] scheme with (9 × 9 × 1) and (3 × 3 × 1) dense k-point meshes. Isolated species in the gas phase were treated by employing a large cell (20 Å × 21 Å × 22 Å) and the Γ point only.

We define the adsorption energy (E_{ads}) as follows

$$E_{ads} = \frac{1}{N_{TAAH}}[E^{total} - E^{Au} - E^{TAAH}] \quad (1)$$

where E^{total}, E^{Au}, E^{TAAH}, and N_{TAAH} stand for the total energy of the system, the energy of the clean surface, the energy of the isolated TAAH, and the number of TAAH species implied in the adsorption process in each model. Negative numbers indicate an exothermic adsorption process with respect to the clean surface and the adsorbates.

RESULTS AND DISCUSSION

Electrochemical desorption is carried out by sweeping the potential from an initial value where the chemisorbed layer is stable up to potentials where the adsorbates are removed from the Au surface. Figure 1a shows typical current density (j) versus potential (E) curves recorded in a 0.1 M NaOH aqueous solution after immersion of the Au(111) substrate in a TAAH 0.1 mM toluene solution for different times (t_i). The presence of broad waves with peak potentials located at E_p = −0.90/−0.95 V in the j versus E profiles can be unambiguously assigned to the desorption of the adsorbed species from the gold surface.

In Figure 1a, it can be seen that the peak potentials (E_p) shifts slightly in the negative direction as t_i increases whereas the charge densities (q) obtained from these desorption curves are roughly equal ($q \approx 107 \pm 10$ μC cm^{-2}) irrespective of the immersion time. The q value can hardly be assigned to a TAA monolayer because the desorption of closely packed arrays of thiol molecules in $(\sqrt{3} \times \sqrt{3})$ R30° or $c(4 \times 2)$ lattices (surface coverage θ = 0.33) according to the reaction

$$RS{-}Au + e = RS^- + Au \quad (2)$$

involves 75 μC cm^{-2}. Also, the peak positions (E_p = −0.95/−0.90 V) are too negative to be related to the desorption of a SAM of a short thiol such as TAAH. In contrast, E_p is observed in the potential window where S desorption from the well-

dx.doi.org/10.1021/la303059u | Langmuir 2012, 28, 15278−15285

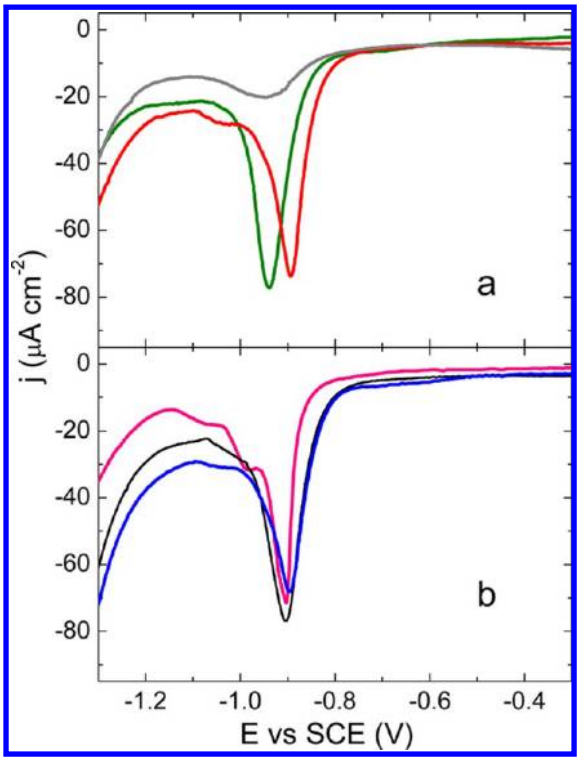

Figure 1. Current density j vs E profiles for the reductive desorption of the adlayer formed by immersion of the Au(111) substrate under different conditions. (a) Five minutes (red) and 12 h (green) in a 0.1 mM solution of TAAH in toluene. The gray curve shows a similar curve after immersion of the Au(111) substrate in 0.1 mM Na_2S in toluene for 5 min. (b) Five minutes in 0.1 mM TAAH in hexane (cyan), ethanol (black), and toluene (blue). Electroreduction curves were recorded in NaOH 0.1 M at a scan rate of 50 mV s^{-1}.

known $(\sqrt{3} \times \sqrt{3})$ R30° lattice (θ = 0.33) takes place by the following reaction[21,22]

$$S{-}Au + 2e \rightarrow S^{2-} + Au \quad (3)$$

Note, however, that S desorption from a $(\sqrt{3} \times \sqrt{3})$ R30° lattice involves q = 150 μCcm^{-2} [2,22−24] rather than q = 107 ± 10 μCcm^{-2}; i.e., the S adlayer seems to be organized in a more diluted surface structure with $\theta \approx 0.25$. This is not surprising because diluted (5 × 5) S lattices with a coverage of θ = 0.28 have already been reported.[25]

We have also carried out electrodesorption experiments from Au substrates that have been immersed in a toluene solution containing sodium sulfide to explore the possible effect of sulfide impurities present in TAAH or some decomposition of this molecule in the solvent (gray curve, Figure 1a). However, the amount of sulfide adsorbed from these solutions is certainly much smaller (q = 28 μC cm^{-2}) than that formed from the TAAH solution (q = 107 μC cm^{-2}). The influence of the solvent in TAAH decomposition was also discarded by using different organic solvents for the self-assembly process (Figure 1b). In fact, in all cases we found E_p (−0.90 ± 0.04 V) and q values (97 to 108 μC cm^{-2}) that are consistent with the presence of S rather than a thiolate SAM but in all cases with q values that were smaller than expected for the $(\sqrt{3} \times \sqrt{3})$ R30° S lattice.

The chemical nature and the surface coverage of the adsorbate have been confirmed by measuring high-resolution photoemission spectra. XP spectra of the S 2p core-level peak from samples prepared by immersion of the Au substrate for 5 min, 1 h, and 12 h in a 0.1 mM TAAH in toluene solution are shown in Figure 2. The observed broad S 2p signals are similar

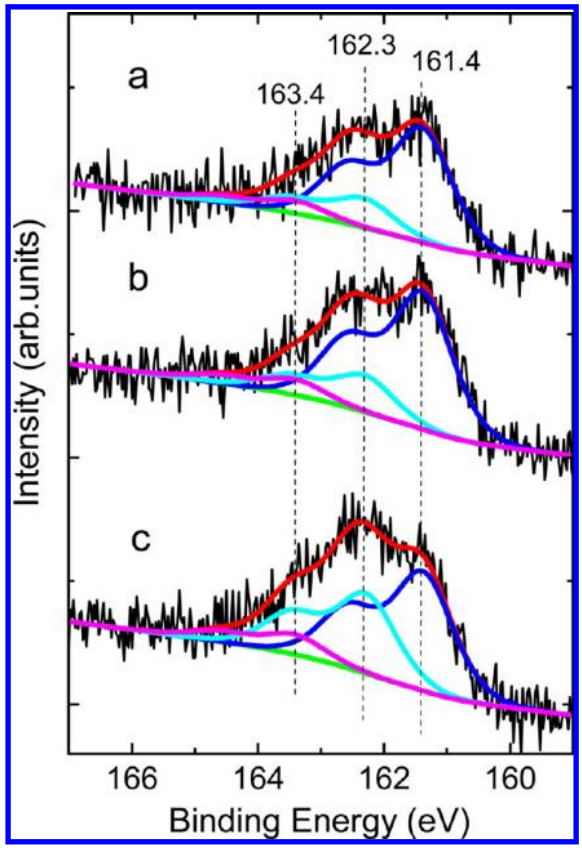

Figure 2. XPS spectra for the S 2p region of a monolayer formed by the immersion of the Au(111) substrate for (a) 5, (b) 60, and (c) 720 min in a 0.1 mM TAAH solution in toluene. Raw data, black; fitted spectra, red; S1 (161.3 eV), blue; S2 (162.2 eV), cyan; S3 (163.3 eV), magenta; Shirley-type background, green.

to those described in the literature for S on Au.[22,26] The experimental data are fitted with three components of the spectra. They have been assigned to atomic (monomeric) chemisorbed S (161.4 eV), polysulfide (polymeric) chemisorbed S (162.3 eV), and S in multilayers not bound to the gold (163.4 eV). The spectra shown in Figure 2 reveal that for all samples the main component is atomic sulfur bound to the gold surface (S1). The coverage of the different S species as a function of the immersion time is shown in Table S1 (Supporting Information) and Figure 3. The surface coverage was obtained from XPS data by normalizing the components of S 2p by the intensity of Au 4f as described in the Experimental Methods section.

In Figure 3, we have also included the total S surface coverage ($\theta_1 + \theta_2 + \theta_3$) of Au substrates immersed in an aqueous 0.1 M NaOH solution containing Na_2S. The analysis of Figure 3 reveals that components θ_1 and θ_3 remain almost constant whereas θ_2 increases with the immersion time (i.e., the Au surface becomes richer in polymeric species at a constant amount of monomeric sulfur). The XPS data taken for 720 min of immersion time also shows that the total surface coverage by monomeric (S1) and polymeric (S2) S species is θ_{1+2} = 0.43. This means that the Au substrate in contact with TAAH cannot reach the surface coverage obtained by S adsorption from

dx.doi.org/10.1021/la303059u | Langmuir 2012, 28, 15278−15285

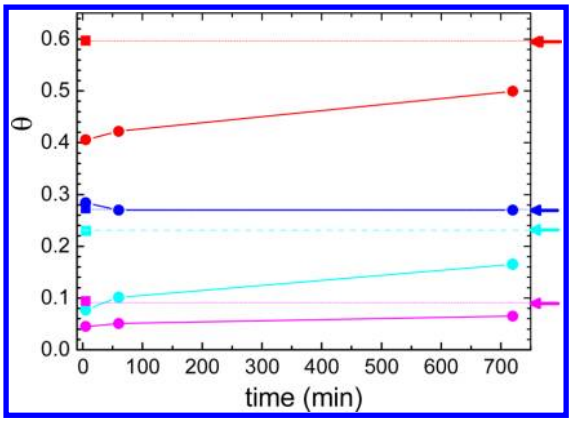

Figure 3. Surface coverage (θ) of monomeric sulfur (blue), polymeric sulfur (cyan), bulk (multilayer) sulfur (magenta), and total sulfur (red) of a TAA SAM. The dashed lines and arrows correspond to the same S 2p components of a SAM formed by immersion for 5 min in an aqueous 0.1 NaOH solution containing 0.1 mM Na_2S.

aqueous Na_2S solutions ($\theta_{1+2} = 0.50$).[27] However, θ_1 (Table S1, Supporting Information) and q, which is related to the reductive desorption of monomeric species by eq 2, are consistent with an amount of monomeric S equivalent to that found in the diluted (5 × 5) S lattice observed in the gas phase ($\theta = 0.28$).[25]

Additional characterization of the monolayer was obtained by STM in order to elucidate the structure formed and compare it with structures already described in the literature. Figure 4

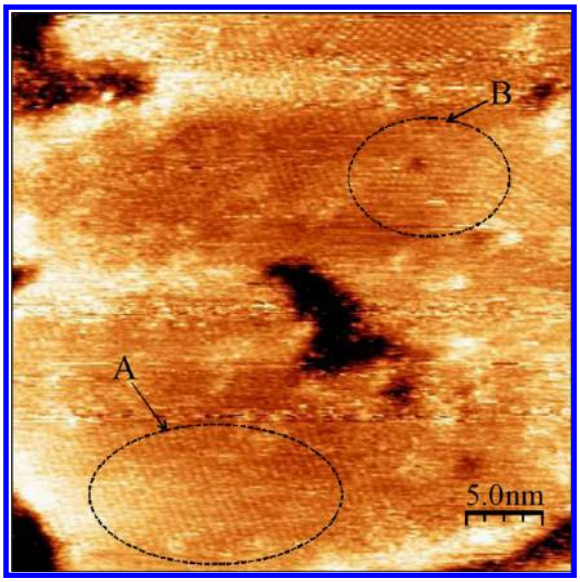

Figure 4. STM image (36 × 36 nm^2) showing the adsorbate structures formed after the immersion of the Au(111) substrate for 1 h in a TAAH 0.1 mM toluene solution. All images presented in this article have been postprocessed using WsXM software (with slope correction and linear interpolation between pixels)[28] (V_{bias} = 500 mV, I_t = 500 pA).

shows a large-area (36 × 36 nm^2) image of the Au substrate after immersion for 1 h in a 0.1 mM TAAH toluene solution. Note that for this time the coverage of S from the XPS analysis is $\theta_{1+2} = 0.38$ (i.e., a mixture of atomic sulfur and polysulfide species is present on the Au surface). In the image, a large terrace with some typical pits resulting from the adsorption of sulfur-containing species is observed. Some regions where atomic resolution is obtained are clearly seen in the image, coexisting with disordered regions. The different domain structures are labeled with letters, denoting regions with parallel straight lines (A) and rectangular structures (B). The rectangular structure labeled B could be assigned to polymeric sulfur on the Au substrate. In fact, surface structures in region B resemble the well-known S rectangles,[5,21,22] consisting of eight atoms of monomeric and polymeric S species formed from Na_2S aqueous solutions or from the decomposition of hexavalent aromatic sulfonyl phthalimide.[5,27]

Figure 5 shows a representative high-resolution STM image (5 × 15 nm^2) of region B. A large single domain of sulfur

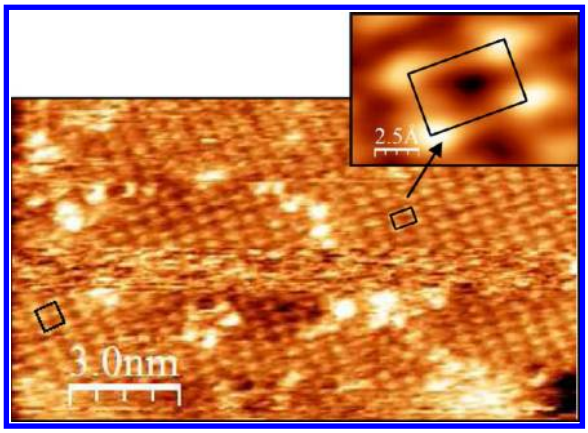

Figure 5. STM image (5 × 15 nm^2) showing the adsorbate structure formed after the immersion of the Au(111) substrate for 1 h in a TAAH 0.1 mM toluene solution. The image shows the atomic resolution of a domain with rectangular structure. (Inset) Enlarged image of the unit cell (rectangle). A rectangle with six S atoms is observed on the left-hand side. (V_{bias} = 500 mV, I_t = 500 pA).

adsorbed on gold with a rectangular structure is clearly seen. The inset in this figure displays a rectangular unit cell with dimensions of (0.33 ± 0.05 nm) × (0.57 ± 0.05 nm), a size compatible with that of the typical S rectangles containing eight S atoms but where two S atoms are missing. The rectangle on the left-hand side of the image points to one of these structures that can be interpreted with the model shown in Figure 6.

In Figure 5, the S rectangle contains six S atoms rather than the eight S units in the typical rectangles already reported.[5,21,22]

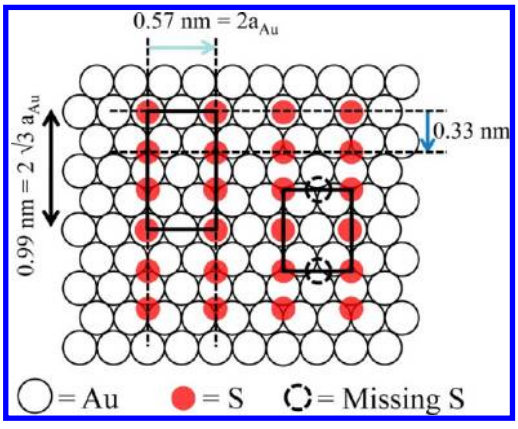

Figure 6. Scheme of the structure adopted by the atoms of the S monolayer on Au(111) based on the STM image of Figure 5.

dx.doi.org/10.1021/la303059u | *Langmuir* 2012, 28, 15278−15285

Because the absence of the two sulfur atoms is observed systematically, the STM image can then be described as a rectangular structure on gold with a unit cell of $2 \times 2\sqrt{3}$ containing three S atoms, with interatomic distances of 0.33 and 0.57 nm. However, A regions exhibit a distance between lines of 0.57 nm, suggesting that they correspond to the same structures observed in B but where no clear atomic resolution inside each line is obtained.

We are proposing that sulfidization of the Au(111) surface in this system involves the initial adsorption of the TAAH species, the cleavage of the S−C bonds, and the formation of a mixture of monomeric S (S1) and polymeric species (S2).

The sulfidization process of the Au(111) substrate should be similar to that observed for this substrate in contact with aqueous sodium sulfide solutions,[21] although in the present system a more diluted S adlayer is produced. In the former case, sulfidization proceeds by the initial formation of a $\sqrt{3} \times \sqrt{3}$ R30° lattice of monomeric S (θ_1 =0.33), which is followed by the formation of rectangular S structures containing monomeric and polymeric S species (θ_{1+2} = 0.50) as more S is incorporated into the surface.[21,26] The experimental data for Au(111) in contact with TAAH suggest that the sulfidization of the Au(111) surface involves the formation of the (5 × 5) S lattice (θ_1 = 0.28), and when more S is produced, the system evolves to the form of polysulfide species (θ_{1+2} = 0.43). In the next section, we will discuss the chemical reactions that could lead to TAAH decomposition to form the (5 × 5) S lattice.

DFT RESULTS

The experimental data clearly show that TAAH decomposes very rapidly to form S species on the Au(111) surface irrespective of the use of polar or nonpolar solvents. Therefore, we propose that both physisorbed TAAH molecule and the Au(111) surface are involved in the formation of the S adlayer.

To understand the energetics of this process, we start modeling TAAH adsorption using a hypothetical unit cell {$(2 \times \sqrt{3})$ (θ = 0.25)} because its complete decomposition results in a surface coverage by monomeric S that is close to the experimental observations (Figure 1 and Table S1 in Supporting Information, θ_1 = 0.28). Note that the $(2 \times \sqrt{3})$ lattice has been observed by STM imaging for thiol adsorption on the Au(111) surface.[29]

The TAAH molecule exhibits two tautomeric forms, thiol ($TAAH_{SH}$) and thione ($TAAH_{OH}$), that can adopt two conformations with respect to the double bond, syn and anti (Figure 7). The DFT calculations show that in the gas phase the syn conformer is more stable than the anti form for both tautomers. However, $TAAH_{SH}$ syn is more stable by 0.14 eV than $TAAH_{OH}$ syn. We have taken the $TAAH_{SH}$ syn molecule as the reference species in the energy calculations.

First we analyze the nondissociative molecular adsorption on the Au(111) surface of the two tautomers in both conformations, syn and anti, in a $(2 \times \sqrt{3})$ overlayer with a coverage of θ = 0.25 (Figure 7a−d). Different adsorption geometries have been studied for these species, but in all cases, the molecules prefer to be adsorbed parallel to the substrate. The higher adsorption energy (E_{ads}) is presented for $TAAH_{OH}$ syn (E_{ads} = −0.63 eV), being ∼−0.04 eV more stable than the $TAAH_{SH}$ species (Table 1). Both conformers prefer to adsorb with S and O atoms on hollow sites. The magnitude of the adsorption energies and the S−Au bond lengths (Table 1) clearly shows that the intact molecules in both tautomeric forms are weakly bound (physisorbed). The physisorption energies are similar to those reported for ethanethiol on the same substrate (E_{ad} = −0.54 eV).[30]

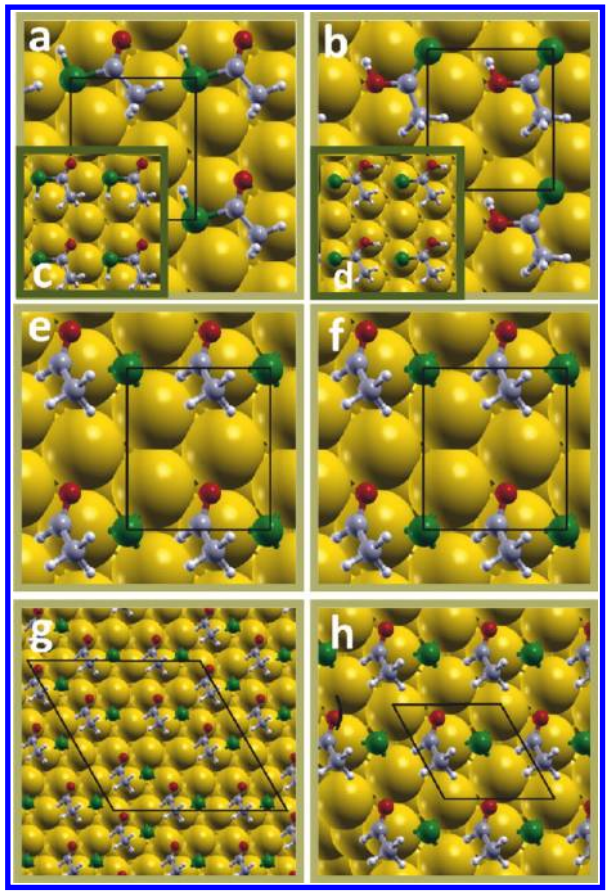

Figure 7. Optimized surface structures: (a) $(2 \times \sqrt{3})$ syn $TAAH_{SH}$, (b) $(2 \times \sqrt{3})$ syn $TAAH_{OH}$, (c) $(2 \times \sqrt{3})$ anti $TAAH_{SH}$, (d) $(2 \times \sqrt{3})$ anti $TAAH_{OH}$, (e) $(2 \times \sqrt{3})$ TAA radical, (f) $(2 \times \sqrt{3})$ S + acetaldehyde, (g) (5 × 5) S + acetaldehyde, and (h) $(\sqrt{3} \times \sqrt{3})$ R30° S + acetaldehyde. Gold, Au; green, sulfur; red, oxygen; gray, carbon; and white: hydrogen.

It is well known that thiols chemisorb on the Au(111) surface by breaking the H−S bond. Therefore, we have also used the chemisorption process with the $(2 \times \sqrt{3})$ unit cell of the TAA radical. The optimized structure is shown in Figure 7e. The bridge-hollow fcc is the most stable site on the surface for the radical species (as it is for alkanethiols) with a S−Au bond length of 2.45 Å. The TAA radical is strongly bound to the Au(111) surface with a binding energy ($E_{binding} = E^{total} - E^{Au} - E^{TAA}$) equal to $E_{binding}$ = −2.33 eV. We have found that a similar binding energy is obtained for butanethiol in the $(\sqrt{3} \times \sqrt{3})$ R30° lattice on the same unreconstructed Au(111) surface when the weak van der Waals interactions are taken into account ($E_{binding}$ = −2.49 eV) using the same calculation procedure (unpublished data). However, it should be noted that chemisorption from the TAAH species yielding TAA + H on the Au(111) surface is an energetically unfavorable process because the adsorption energy is E_{ads} = +0.28 eV.

The geometrical parameters and Bader charges of the chemisorbed TAA radical are also similar to those estimated for chemisorbed alkanethiols, giving no structural evidence to understand the S−C bond-breaking tendency of the adsorbed TAA that results in the complete sulfidization of the Au(111) surface.

dx.doi.org/10.1021/la303059u | Langmuir 2012, 28, 15278−15285

Table 1. Calculated Adsorption Energies, Bond Lengths, and Bader Charges for the Studied Models

model	adsorption energy (E_{ads})/eV	Au−S vertical distance/Å	S−C bond length/Å	Bader charge/e		
				S	C	Au
$TAAH_{OH}$ syn	−0.63	2.89	1.65	+1.37	−0.52	−0.03
$TAAH_{SH}$ syn	−0.59	3.31	1.78	+0.04	+1.66	−0.02
$TAAH_{OH}$ anti	−0.50	2.65	1.66	+1.32	−0.47	−0.02
$TAAH_{SH}$ anti	−0.47	2.68	1.78	+0.08	+1.24	−0.03
TAA + H	+0.28	1.90	1.83	−0.16	+1.7	+0.04
[S + AA] $(2 \times \sqrt{3})$	−0.72	1.56		−0.31	+1.98	+0.080
[S + AA] (5×5)	−1.06	1.56		−0.26	+1.98	+0.084
[S + AA] $(\sqrt{3} \times \sqrt{3})$ R30°	−0.76	1.55		−0.27	+1.98	+0.095

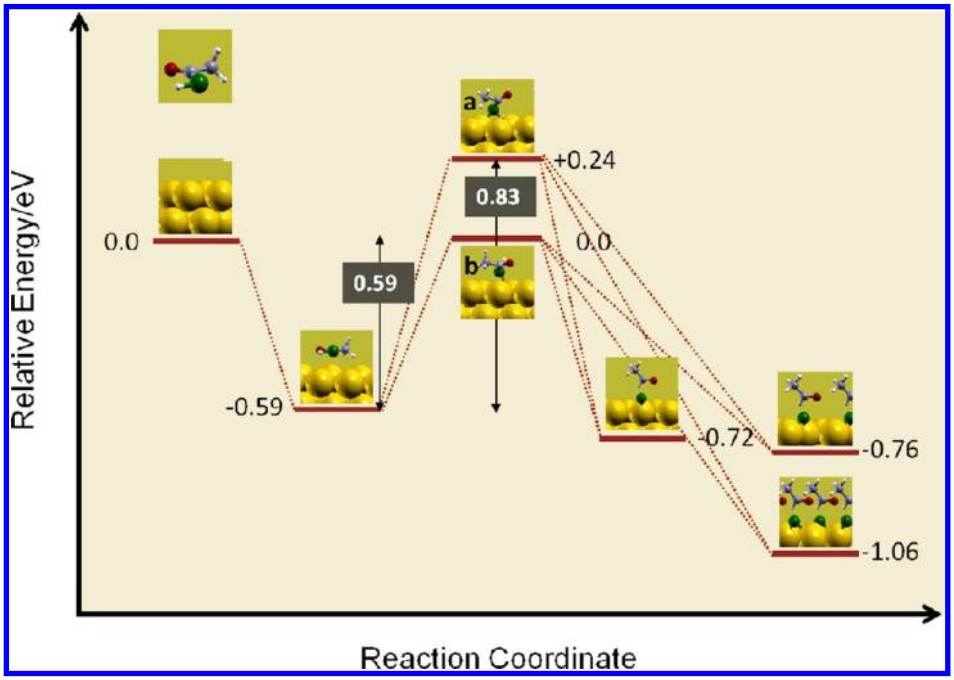

Figure 8. Energy paths of S adlayer formation from the TAAH molecule adsorbed on the Au(111) surface.

We have also estimated the adsorption energy of a S + acetaldehyde (AA) mixture on different unit cells on Au(111) (i.e., $(2 \times \sqrt{3})$, (5×5), and $(\sqrt{3} \times \sqrt{3})$ R30°; Figure 7f–h) in order to gain insight into the experimental sulfidization of the system. We found adsorption energies of −0.72, −1.06, and −0.76 eV, respectively, suggesting that the S−C bond breaking yielding S + AA is energetically favored for the (5×5) S adlayer.

Now we discuss the possible mechanism for S adlayer formation on the Au(111) surface. We propose two different reaction pathways as shown in Figures 8 and 9. In the first mechanism (a), we start with the physisorbed TAAH species on the Au(111) surface. Then the H−S homolytic cleavage bond forms, yielding the chemisorbed TAA radical that binds to the Au(111) surface (Figure 9a) through the S atom at the hollow fcc position. However, the H atom released from H−S bond dissociation chemisorbs first at the neighboring hollow hcp site and then diffuses on the surface to reach the top site closer to the carbonyl C atom. It is well known that the difference in energy for H adsorption between different sites on the Au(111) surface is small enough to permit adsorbed H to move almost freely on the Au(111) surface.[31] Bader charge analysis shows that the adsorbed H has excess negative charge (hydride behavior) that favors its bonding to the carbonyl carbon atom through a nucleophilic attack (Figure 9a) leaving S on the surface and releasing an acetaldehyde molecule. This mechanism involves an activation energy barrier, E_a = +0.83 eV, that corresponds to the cleavage of the strong S−H bond. Similar energy barriers have been found for alkanethiol chemisorption on the Au(111) surface.[32] In fact, the route to hydrogen removal is considered be an important parameter influencing the formation kinetics, structure, and stability of SAMs of thiols on Au(111). Values of $E_a \approx +1.0$ eV have been estimated for methanethiolate SAM formation from methanethiol,[33] a process that is too slow to be experimentally observed.

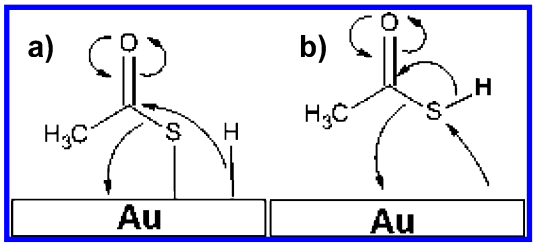

Figure 9. Scheme for two possible mechanisms (a and b) proposed to explain the S adlayer formation.

dx.doi.org/10.1021/la303059u | Langmuir 2012, 28, 15278−15285

The second mechanism (mechanism b) also starts with the TAAH physisorption to the Au(111) surface. However, in this reaction mechanism the H atom does a 1, 2 shift to the carbonyl carbon atom, producing a transient quasi-tetrahedrical intermediate that evolves to the final products (Figure 9b) (i.e., chemisorbed S + AA through a concerted process). The AA product is initially physisorbed, but it is then displaced from the Au(111) surface by other arriving TAAH molecules during the self-assembly process to form a dense S adlayer as it is experimentally found. The barrier energy calculated for this mechanism is E_a = +0.59 eV (Figure 8) (i.e., a lower activation energy barrier than that estimated for mechanism a). Therefore, the sulfidization reaction should proceed faster by mechanism b.

Then, the sulfidization process of the Au(111) surface can be formulated by the following mechanism (Figure 8 b), assuming E_a = +0.59 eV to reach the transition state (TS) and a final stabilization of −0.34 eV in going from the $(2 \times \sqrt{3})$ S to the (5×5) S adlayer.

$$\mathrm{TAAH} + \mathrm{Au(111)} \rightarrow \mathrm{TAAH_{phys}/Au(111)}$$
$$E_{react} = -0.59\ \mathrm{eV}$$

$$\mathrm{TAAH_{phys}/Au(111)} \rightarrow \mathrm{TAAH_{chem..}/Au(111)_{TS}}$$
$$E_{react} = +0.59\ \mathrm{eV}$$

$$\mathrm{TAAH_{chem}/Au(111)_{TS}} \rightarrow [\mathrm{S_{chem}} + \mathrm{AA_{phys}}]_{2\times\sqrt{3}}/\mathrm{Au(111)}$$
$$E_{react} = -0.72\ \mathrm{eV}$$

$$7[\mathrm{S_{chem}} + \mathrm{AA_{phys}}]_{2\times\sqrt{3}}/\mathrm{Au(111)} \rightarrow [7\mathrm{S_{chem}} + 7\mathrm{AA_{phys}}]_{(5\times5)}/\mathrm{Au(111)}$$
$$E_{react} = -0.34\ \mathrm{eV}$$

Note that the value of E_{ads} = +0.59 eV is similar to that found for dimethyl disulfide adsorption on Au(111), a process that proceeds at room temperature to yield a self-assembled monolayer of methanethiolate.[34] The decrease in E_{ads} in mechanism b with respect to that in mechanism a can be related to the H-atom exchange between H−S and C═O groups. Indeed, an intermolecular hydrogen atom exchange has recently been proposed as a key step in thiol adsorption with a lower energy barrier.[33]

CONCLUSIONS

We have found that the TAAH molecule adsorbs on Au(111), leading to sulfidization irrespective of the solvent used in the self-assembly process. The S layer is composed of monomeric and polymeric S with a coverage lower than that found for Au(111) sulfidization from aqueous solutions containing sodium sulfide. We propose a mechanism that favors S and acetaldehyde formation involving a hydride transfer from the S−H bond to the O atom mediated by the carbonyl group and the Au(111) surface. The TAAH adsorption reveals the strong effect that produces a functional group and the key role of the S−H bond cleavage in the self-assembly process.

ASSOCIATED CONTENT

Supporting Information

The tautomeric equilibrium of the two forms of the TAAH molecule. Surface coverages for S species obtained from XPS for Au(111) surfaces immersed for different times in toluene solutions. This material is available free of charge via the Internet at http://pubs.acs.org.

AUTHOR INFORMATION

Corresponding Author

*(A.A.P.) E-mail: pasa@fisica.ufsc.br. Phone/Fax: 0055 48 234-0599. (M.E.V.) E-mail: mevela@inifta.unlp.edu.ar. Phone: +54 221 4257430. Fax: +54 221 4254642 Website: http//nano.quimica.unlp.edu.ar.

Notes

The authors declare no competing financial interest.

ACKNOWLEDGMENTS

We acknowledge support from ANPCyT (Argentina, PICT-2010-2554, PICT-CNPQ 08-0019), CONICET (Argentina, PIP 11220090100139), MICINN (Spain CTQ2011-27484), ACIISI (Canarias, ID20100152), CNPQ (proc. 490636/2008-0), CAPES, and FAPESC (Brazil). M.E.V. is a member of the research center of CIC, BsAs, Argentina.

REFERENCES

(1) Creczynski-Pasa, T. B.; Daza Millone, M. A.; Munford, M. L.; de Lima, V. R.; Vieira, T. O.; Benitez, G. A.; Pasa, A. A.; Salvarezza, R. C.; Vela, M. E. Self-assembled dithiothreitol on Au surfaces for biological applications: phospholipid bilayer formation. *Phys. Chem. Chem. Phys.* **2009**, *11*, 1077−1084.

(2) Vericat, C.; Vela, M. E.; Benitez, G.; Carro, P.; Salvarezza, R. C. Self-assembled monolayers of thiols and dithiols on gold: new challenges for a well-known system. *Chem. Soc. Rev.* **2010**, *39*, 1805−1834.

(3) Love, J. C.; Estroff, L. A.; Kriebel, J. K.; Nuzzo, R. G.; Whitesides, G. M. Self-assembled monolayers of thiolates on metals as a form of nanotechnology. *Chem. Rev.* **2005**, *105*, 1103−1169.

(4) Ulman, A. Formation and structure of self-assembled monolayers. *Chem. Rev.* **1996**, *96*, 1533−1554.

(5) Koczkur, K. M.; Hamed, E. M.; Hesp, C. R.; Houmam, A. Gold catalyzed reduction of a hexavalent aromatic sulfonyl phthalimide to sulfur. *Chem. Commun.* **2011**, *47*, 12128−12130.

(6) Koczkur, K. M.; Hamed, E. M.; Houmam, A. Sulfur multilayer formation on Au(111): new insights from the study of hexamethyldisilathiane. *Langmuir* **2011**, *27*, 12270−12274.

(7) Kycia, A. H.; Sek, S.; Su, Z. F.; Merrill, A. R.; Lipkowski, J. Electrochemical and STM studies of 1-thio-beta-D-glucose self-assembled on a Au(111) electrode surface. *Langmuir* **2011**, *27*, 13383−13389.

(8) Cometto, F. P.; Macagno, V. A.; Paredes-Olivera, P.; Patrito, E. M.; Ascolani, H.; Zampieri, G. Decomposition of methylthiolate monolayers on Au(111) prepared from dimethyl disulfide in solution phase. *J. Phys. Chem. C* **2010**, *114*, 10183−10194.

(9) Iwahori, K.; Yamashita, I. Fabrication of CdS nanoparticles in the bio-template, apoferritin cavity by a slow chemical reaction system. *J. Phys.: Conf. Ser.* **2007**, *61*, 492.

(10) Perdew, J. P.; Chevary, J. A.; Vosko, S. H.; Jackson, K. A.; Pederson, M. R.; Singh, D. J.; Fiolhais, C. Atoms, molecules, solids, and surfaces: applications of the generalized gradient approximation for exchange and correlation. *Phys. Rev. B* **1992**, *46*, 6671−6687.

(11) Blöchl, P. E. Projector augmented-wave method. *Phys. Rev. B* **1994**, *50*, 17953−17979.

(12) Blöchl, P. E.; Margl, P.; Schwarz, K. Ab Initio Molecular Dynamics with the Projector Augmented Wave Method. In *Chemical Applications of Density-Functional Theory*; Laird, B. B., Ross, R. B., Ziegler, T., Eds.; American Chemical Society: Washington, DC, 1996; Vol. *629*, pp 54−69.

(13) Kresse, G.; Joubert, D. From ultrasoft pseudopotentials to the projector augmented-wave method. *Phys. Rev. B* **1999**, *59*, 1758−1775.

(14) Kresse, G.; Furthmüller, J. Efficient iterative schemes for ab initio total-energy calculations using a plane-wave basis set. *Phys. Rev. B* **1996**, *54*, 11169−11186.

(15) Grimme, S. Semiempirical GGA-type density functional constructed with a long-range dispersion correction. *J. Comput. Chem.* **2006**, *27*, 1787−1799.
(16) Sławińska, J.; Dabrowski, P.; Zasada, I. Doping of graphene by a Au(111) substrate: calculation strategy within the local density approximation and a semiempirical van der Waals approach. *Phys. Rev. B* **2011**, *83*, 245429.
(17) Toyoda, K.; Hamada, I.; Lee, K.; Yanagisawa, S.; Morikawa, Y. Density functional theoretical study of pentacene/noble metal interfaces with van der Waals corrections: vacuum level shifts and electronic structures. *J. Chem. Phys.* **2010**, *132*, 134703.
(18) Jónsson, H. Theoretical studies of atomic-scale processes relevant to crystal growth. *Annu. Rev. Phys. Chem.* **2000**, *51*, 623−653.
(19) Henkelman, G.; Uberuaga, B. P.; Jónsson, H. A climbing image nudged elastic band method for finding saddle points and minimum energy paths. *J. Chem. Phys.* **2000**, *113*, 9901−9904.
(20) Monkhorst, H. J.; Pack, J. D. Special points for Brillouin-zone integrations. *Phys. Rev. B* **1976**, *13*, 5188−5192.
(21) Vericat, C.; Andreasen, G.; Vela, M. E.; Salvarezza, R. C. Dynamics of potential-dependent transformations in sulfur adlayers on Au(111) electrodes. *J. Phys. Chem. B* **2000**, *104*, 302−307.
(22) Vericat, C.; Vela, M. E.; Andreasen, G.; Salvarezza, R. C.; Vázquez, L.; Martin-Gago, J. A. Sulfur-substrate interactions in spontaneously formed sulfur adlayers on Au(111). *Langmuir* **2001**, *17*, 4919−4924.
(23) Hamilton, I. C.; Woods, R. An investigation of the deposition and reactions of sulfur on gold electrodes. *J. Appl. Electrochem.* **1983**, *13*, 783−794.
(24) Vericat, C.; Andreasen, G.; Vela, M. E.; Martin, H.; Salvarezza, R. C. Following transformation in self-assembled alkanethiol monolayers on Au(111) by in situ scanning tunneling microscopy. *J. Chem. Phys.* **2001**, *115*, 6672−6678.
(25) Yu, M.; Ascolani, H.; Zampieri, G.; Woodruff, D. P.; Satterley, C. J.; Jones, R. G.; Dhanak, V. R. The structure of atomic sulfur phases on Au(111). *J. Phys. Chem. C* **2007**, *111*, 10904−10914.
(26) Rodriguez, J. A.; Dvorak, J.; Jirsak, T.; Liu, G.; Hrbek, J.; Aray, Y.; Gonzalez, C. Coverage effects and the nature of the metal-sulfur bond in S/Au(111): High-resolution photoemission and density-functional studies. *J. Am. Chem. Soc.* **2003**, *125*, 276−285.
(27) Lustemberg, P. G.; Vericat, C.; Benitez, G. A.; Vela, M. E.; Tognalli, N.; Fainstein, A.; Martiarena, M. L.; Salvarezza, R. C. Spontaneously formed sulfur adlayers on gold in electrolyte solutions: Adsorbed sulfur or gold sulfide? *J. Phys. Chem. C* **2008**, *112*, 11394−11402.
(28) Horcas, I.; Fernandez, R.; Gomez-Rodriguez, J. M.; Colchero, J.; Gomez-Herrero, J.; Baro, A. M. WSXM: a software for scanning probe microscopy and a tool for nanotechnology. *Rev. Sci. Instrum.* **2007**, *78*, 013705.
(29) Vericat, C.; Vela, M. E.; Salvarezza, R. C. Self-assembled monolayers of alkanethiols on Au(111): surface structures, defects and dynamics. *Phys. Chem. Chem. Phys.* **2005**, *7*, 3258−3268.
(30) Yourdshahyan, Y.; Rappe, A. M. Structure and energetics of alkanethiol adsorption on the Au(111) surface. *J. Chem. Phys.* **2002**, *117*, 825−833.
(31) Fan, X.; Chi, Q.; Liu, C.; Lau, W. From nondissociative to dissociative adsorption of benzene-thiol on Au(111): a density functional theory study. *J. Phys. Chem. C* **2011**, *116*, 1002−1011.
(32) Grönbeck, H.; Curioni, A.; Andreoni, W. Thiols and disulfides on the Au(111) surface: the headgroup−gold interaction. *J. Am. Chem. Soc.* **2000**, *122*, 3839−3842.
(33) Askerka, M.; Pichugina, D.; Kuz'menko, N.; Shestakov, A. Theoretical prediction of S−H bond rupture in methanethiol upon interaction with gold. *J. Phys. Chem. A* **2012**, *116*, 7686−7693.
(34) Jaccob, M.; Rajaraman, G.; Totti, F. On the kinetics and thermodynamics of S−X (X = H, CH_3, SCH_3, $COCH_3$, and CN) cleavage in the formation of self-assembled monolayers of alkylthiols on Au(111). *Theor. Chem. Acc.* **2012**, *131*, 1−11.